

Electrolyte-Based On-Demand and Disposable Microbattery

Ki Bang Lee and Liwei Lin, *Member, IEEE, Member, ASME*

Abstract—A micromachined battery based on liquid electrolyte and metal electrodes for on-demand and disposable usages has been successfully demonstrated. The microbattery uses gold as the positive electrode and zinc as the negative electrode and is fabricated by using the standard surface micromachining technology. Two kinds of electrolytes have been tested, including the combination of sulfuric acid/hydrogen peroxide and potassium hydroxide. The operation of the battery can be on-demand by putting a droplet of electrolyte to activate the operation. Theoretical voltage and capacity of the microbattery are formulated and compared with experimental results. The experimental study shows that a maximum voltage of 1.5 V and maximum capacity of 122.2 $\mu\text{W}\cdot\text{min}$ have been achieved by using a single droplet of about 0.5 μl of sulfuric acid/hydrogen peroxide. [848]

Index Terms—Battery, disposable micropower, MEMS, micro-machines, microsystems.

I. INTRODUCTION

MICROPOWER generation aiming at generating power directly from microstructures may greatly impact the application and architecture of microsystems. Various approaches to supply power for microscale devices are now being investigated to enable standalone microsensors, actuators and future nanostructures for various types of functionalities. The advantages of these MEMS systems are severely limited by the associated bulky batteries and the capability of providing power source may well be the bottleneck for nanostructures. Some of the initial demonstrations on microfuel cells research have shown very promising results toward the concept of “macropower from micromachinery” [1]. Most of these projects use hydrogen, oxygen and other fuels to generate microcombustion and target 10 to 100 W of continuous power supply and aim to have better fuel efficiency [2]. However, in order to fabricate the combustion chambers or fuel cells for these micropower sources, it generally requires complicated micromachining processes. For example, MIT’s microturbine project uses a six-wafer bonding process that is not compatible with most of the other MEMS processes [3]. Furthermore, the manufacturing cost for these micropower sources appears to be high and may not be competitive economically.

On the other hand, a low cost, high capacity microbattery is desirable for MEMS devices [4]–[6]. Previously, solar cells

Manuscript received April 9, 2002; revised May 31, 2003. This work was supported in part by a DARPA/MTO/BioFlips grant. This paper was presented in part at the 15th IEEE Micro Electro Mechanical Systems Conference, Las Vegas, NV, January 2002. Subject Editor D.-I. Cho.

The authors are with the Berkeley Sensor and Actuator Center, Department of Mechanical Engineering, University of California at Berkeley, Berkeley, CA 94720-1740 USA (e-mail: kblee@me.berkeley.edu).

Digital Object Identifier 10.1109/JMEMS.2003.820272

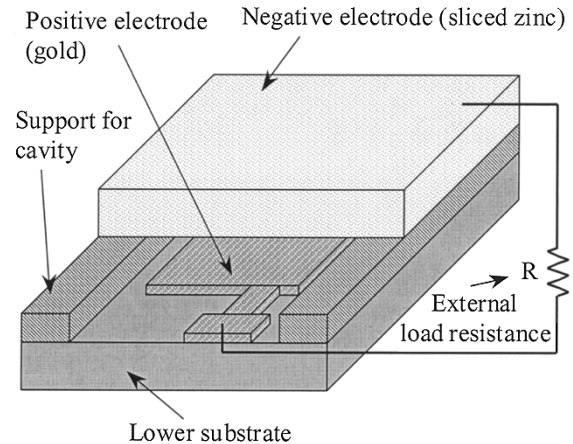


Fig. 1. Schematic of an electrolyte on-demand and disposal microbattery: both positive electrode (gold) and supports for forming the electrolyte cavity are placed on the lower substrate while the negative electrode (zinc) is capped; the microbattery works after putting liquid electrolyte (see Fig. 2).

[7] and rechargeable microbatteries [8]–[11] have been investigated by using rather complicated micromachining processes. Furthermore, drawbacks can be identified among these microbatteries. For example, rechargeable microbattery with KOH liquid electrolyte suffers from the self-discharge effect even if the battery is not in use such that it has short shelf life [8], [9]. Rechargeable thin-film microbatteries commonly use solid electrolytes but their manufacturing processes are generally not compatible with the conventional integrated circuits (ICs) fabrication processes [10], [11]. The disposable microbattery presented in this paper is compatible with IC processing and can be activated by adding the liquid electrolyte on-demand to supply power. Although the power efficiency may not be great in this prototype demonstration as compared with the state-of-art battery technology, it has good potential for disposable devices where only limited power supply is required for limited operation and efficiency is not a big concern. For example, disposable microsystems such as diagnostic devices, DNA chips, Labs-on-a-Chip, and even disposable microtransceivers will be best equipped with an on-demand, disposable microbattery that could provide limited power suitable for the lifetime of the microdevices.

II. MICROBATTERY THEORY

Fig. 1 illustrates the schematic diagram of the electrolyte based, on-demand and disposable microbattery which consists of a positive electrode (gold), a negative electrode (zinc), and an electrolyte cavity. A pair of supports is used to form the cavity between the positive and negative electrodes. The

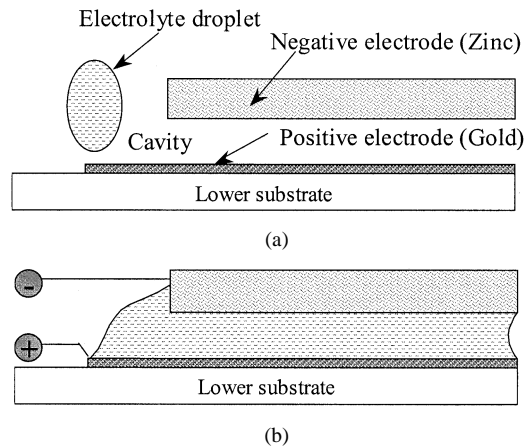
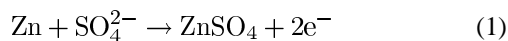


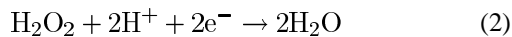
Fig. 2. Working principle of the microbattery: (a) upon putting a liquid-electrolyte droplet in front of the cavity, the electrolyte penetrates into the cavity by surface tension and (b) the microbattery works to supply power.

operation of the microbattery is on-demand by putting a droplet of electrolyte in front of the cavity as shown in Fig. 2. Surface tension force drives the electrolyte into and fill up the cavity quickly to power to an external load, by electro-chemical reaction. Electrons, generated at the negative electrode (zinc), flow through the load resistor as shown in Fig. 1 and are collected at the positive electrode (gold). In this preliminary demonstration, the combination of sulfuric acid (H_2SO_4) and hydrogen peroxide (H_2O_2) is chosen as the liquid electrolyte. The sulfuric acid and hydrogen peroxide are chosen because they can be easily obtained and mixed up as the electrolyte for experiments. Hydrogen peroxide is added to assist removing hydrogen gas in the electrochemical reaction. It is noted that gold is the electron collector and is not reactive in the process.

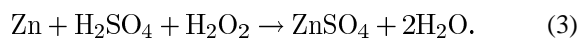
The electrochemical reactions of the microbattery at the zinc electrode can be expressed as the anodic reaction (oxidation)



the cathodic reaction (reduction) is represented as



and the overall reaction is



It is observed from (1)–(3) that the electrons flow through the external load resistor and ions of H^+ and SO_4^{2-} flow within the electrolyte, inside the cavity. The theoretical voltage can be obtained from the change in the Gibbs free energy between reactants and products as follows [12]

$$V^\circ = \frac{-\Delta G^\circ}{nF} \quad (4)$$

where V° , ΔG° , n and F denote the standard voltage, the change in the Gibbs free energy at the standard state, the number of moles of the changed electrons during the reaction, and Faraday defined by 96 500 Coulombs, respectively. The

TABLE I
GIBBS FREE ENERGIES AND WEIGHTS OF THE CHEMICALS

	Chemical	ΔG° [kJ/mol]	Weight [g/mol]
Reactants	Zn	0 (definition)	65.37
	H_2SO_4	-744.53	98.08
	H_2O_2	-120.35	34.02
Products	ZnSO_4	-891.59	161.43
	H_2O	-228.57	18.02

Gibbs free energy change of the reaction in (4) can be written as [13]

$$\Delta G^\circ = \Sigma(\Delta G^\circ)_p - \Sigma(\Delta G^\circ)_r \quad (5)$$

where subscripts p and r indicate products and reactants in (3), respectively. Using (4)–(5) and the Gibbs free energy in Table I, the standard voltage, V° , in the case of tested microbattery is calculated as $V^\circ = 2.5$ V.

In order to obtain the theoretical capacity of the microbattery, electrons per mole of the reactants are used. From (1) and (2), two moles of electrons move from the anode (Zn) to the cathode (H_2O_2) through the external load resistor when one mole of each reactant consumes as shown in (3). Therefore the theoretical electron capacity (Columb/g), E_{cap} , can be expressed as follows:

$$E_{\text{cap}} = \frac{nF}{\text{total molar mass of active components}}. \quad (6)$$

The theoretical capacity is calculated from (6) and the data of Table I as $E_{\text{cap}} = 0.271$ Ah/g. The gravimetric energy density (Wh/g) is obtained as $E_g = V^\circ E_{\text{cap}} = 0.678$ Wh/g. The theoretical voltage and capacity of this microbattery using zinc, sulfuric acid, and hydrogen peroxide are 2.5 V and 0.271 Ah/g that are comparable to those of 2.8 V and 0.271 Ah/g of the magnesium battery [12].

III. FABRICATION

The disposable microbattery has been designed and fabricated by a standard surface micromachining process [14]. The process starts with the growth of a $0.6\text{-}\mu\text{m}$ -thick low stress low-pressure chemical vapor deposition (LPCVD) silicon nitride layer on the silicon substrate as an electric isolation layer. In the processing step of Fig. 3(a), a $0.5\text{-}\mu\text{m}$ -thick LPCVD polysilicon (poly0) is deposited and patterned for the basis of the electrolyte cavity support. A $2\text{-}\mu\text{m}$ -thick sacrificial PSG (phosphosilicate glass) layer is deposited in the step of Fig. 3(b). Fig. 3(c) shows that a $2\text{-}\mu\text{m}$ -thick polysilicon (poly1) is deposited and patterned for constructing the support. Afterwards, a $0.75\text{-}\mu\text{m}$ -thick PSG2 layer is deposited and patterned as shown in Fig. 3(d). A LPCVD $1.5\text{-}\mu\text{m}$ -thick polysilicon (poly2) is deposited and patterned for the positive electrode and the support in Fig. 3(e). A $0.5\text{-}\mu\text{m}$ -thick gold layer for positive electrode and contact pads is then deposited and patterned using lift-off in the processing step of Fig. 3(f). After the removal [see Fig. 3(g)] of the sacrificial PSG layers using HF solution to construct the electrolyte cavity, the microbattery is rinsed and dried. The process is completed by bonding a sliced piece of zinc on the top of the silicon substrate [15] of microbattery

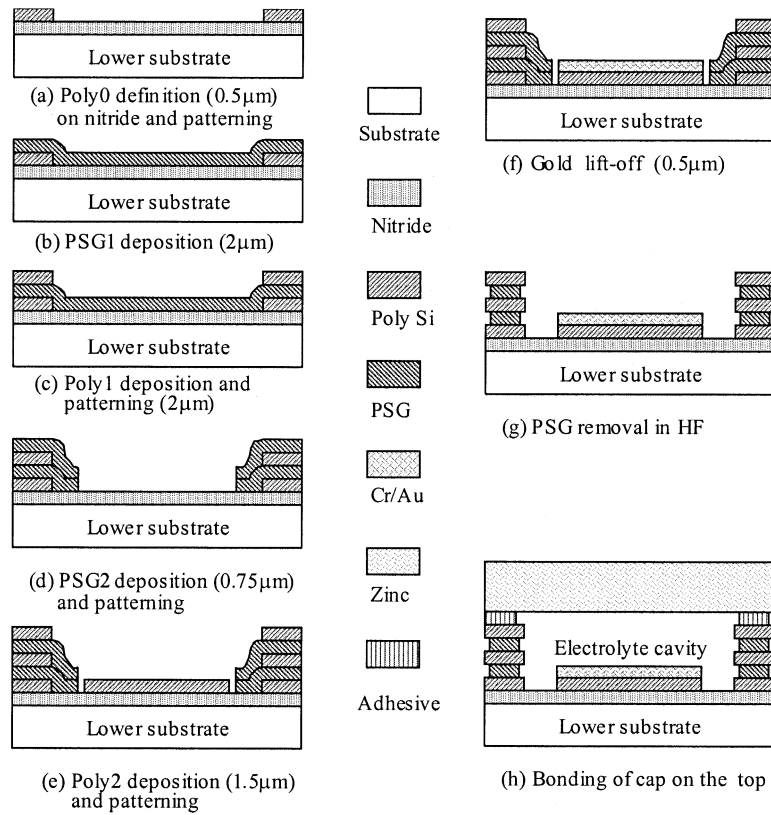


Fig. 3. Fabrication process for the microbattery.

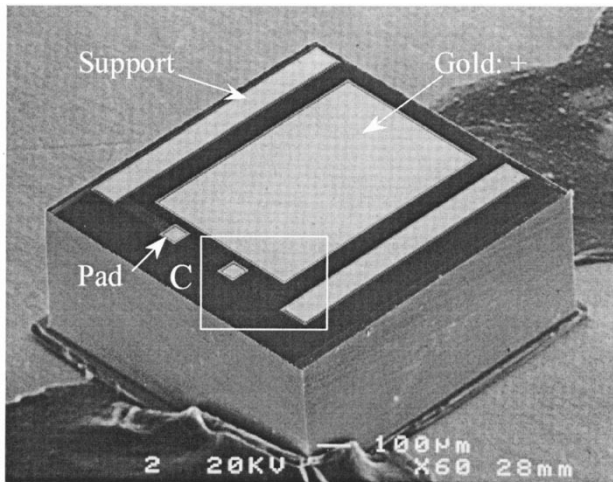


Fig. 4. SEM photograph of a fabricated microbattery before capping: the size is $1\text{ mm} \times 1\text{ mm}$.

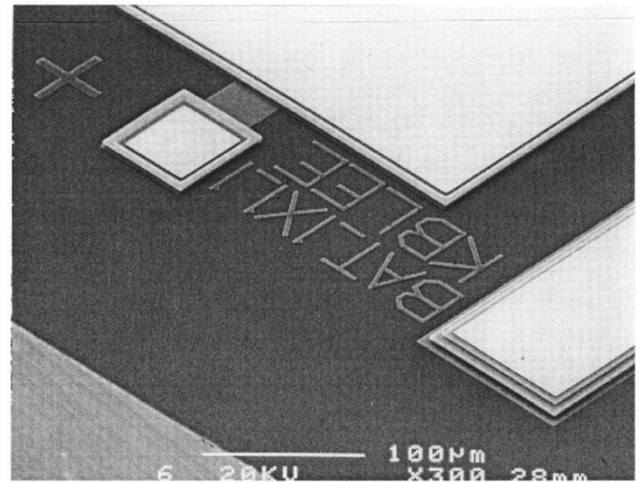


Fig. 5. Close view of *C* in Fig. 4 showing the positive electrode (gold), a pad and the cavity support.

or using adhesive for bonding as shown in Fig. 3(h). Fig. 4 shows a scanning electron microscope (SEM) photograph of the fabricated microbattery right after the process step of Fig. 3(g) and the chip area is $1\text{ mm} \times 1\text{ mm}$. Gold electrode with an area of $600\text{ }\mu\text{m} \times 850\text{ }\mu\text{m}$ and two cavity supports are constructed as shown. Fig. 5 is a close view of area *C* in Fig. 4 showing a contact pad, part of cavity support and part of gold layer used for the positive electrode. Fig. 6 shows the SEM photograph of capped microbattery before putting a droplet of the electrolyte. The cap substrate, cavity and wires for experimental measurement are also shown.

IV. RESULTS AND DISCUSSIONS

The output voltage of the microbattery has been measured with respect to time for various combinations of electrolyte concentration and load resistors at $20\text{ }^\circ\text{C}$. After placing a droplet of $0.5\text{ }\mu\text{l}$ in front of the cavity (see Fig. 2), voltage has been measured by a voltmeter. The molarity of the hydrogen peroxide is set at 10% higher than that of the sulfuric acid in order to minimize the generation of hydrogen gas in all experiments.

Figs. 7–10 shows the measured voltages of the microbattery when changing the concentration of sulfuric acid and the load

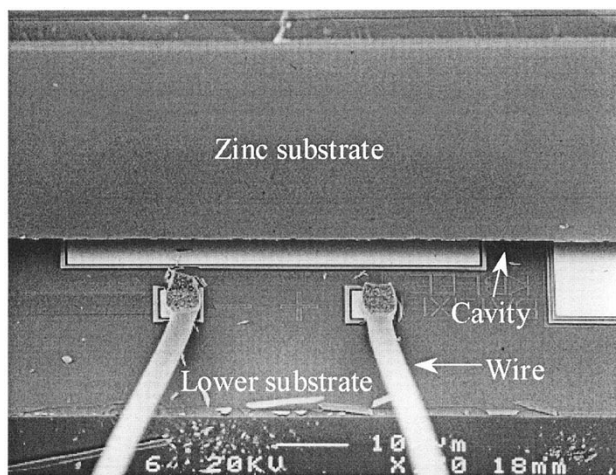


Fig. 6. SEM photograph of capped microbattery before putting the electrolyte.

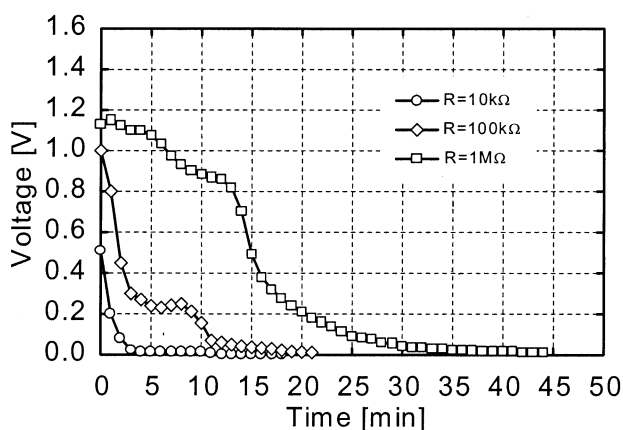


Fig. 7. Measured voltage of the microbattery with 0.5 M sulfuric acid.

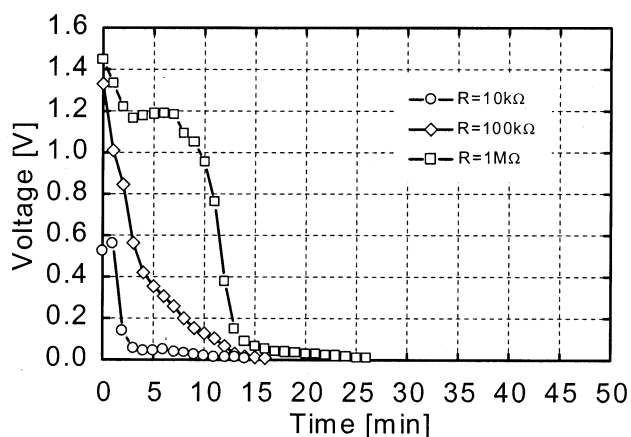


Fig. 8. Measured voltage of the microbattery with 1.0 M sulfuric acid.

resistance. It is noted from Figs. 7–9 that higher concentration of sulfuric acid results in higher voltage output, and higher load resistance results in longer service time but smaller output current. In Fig. 10, the service period of the 2.0 M (Mole/liter) sulfuric acid is shorter than that of the 1.5 M sulfuric acid in Fig. 9 due to the generation of hydrogen bubbles in the electrolyte. It is observed from Fig. 9 that the measured maximum voltage of this microbattery is 1.5 V in the case of 1.5 M sulfuric acid with a load resistance of 1 MΩ. Although the measured voltage of

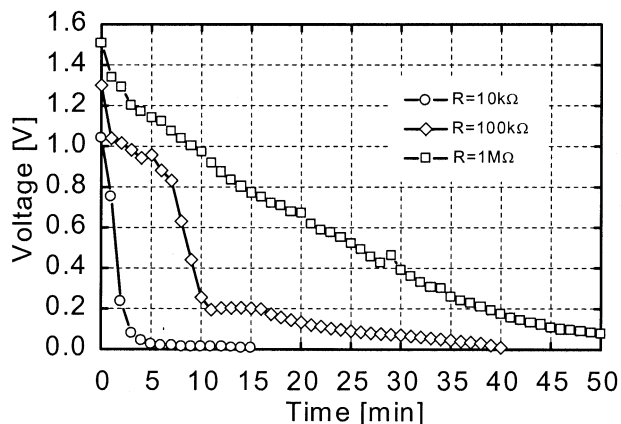


Fig. 9. Measured voltage of the microbattery with 1.5 M sulfuric acid.

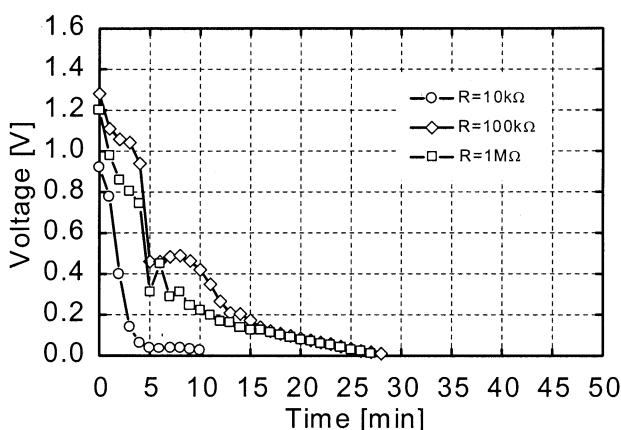


Fig. 10. Measured voltage of the microbattery with 2.0 M sulfuric acid, where bubble generation is observed.

1.5 V is less than the theoretical voltage of 2.5 V, obtained from (4) and (5), it could be sufficient to drive low voltage microelectronics. The service time of this prototype microbattery that has voltage output over 1.0 V is approximately 10 minutes in Figs. 8 and 9 when using the resistance of 1 MΩ and sulfuric acid molarity of 1 M and 1.5 M with a single droplet of electrolyte.

Fig. 11 is a battery model [12] that qualitatively explains the output voltage reaction by Kirchoff's law

$$V = V^o - V_{oe} - V_{os} - E_p = RI \tag{7}$$

where V_{oe} is the ohmic drop in the electrodes, V_{os} is the ohmic drop in the solution, E_p is the voltage drop due to reactions at the electrode/solution interface, and the current flowing through the load resistor. The magnitude of E_p depends on a number of effects, including charge transfer, nucleation and growth of phases or availability of reacting species. In order to maximize the output voltage, several approaches can be used to minimize V_{oe} and V_{os} such as 1) to lessen the anode/cathode gap to lower V_{os} ; 2) to ensure adequate electrode conductivity to lower V_{oe} ; and 3) to optimize the connections to electrodes to lower V_{oe} . The current can be represented by substituting $V_{oe} = R_{oe}I$ and $V_{os} = R_{os}I$ into (7) as

$$I = \frac{V^o - E_p}{R + R_{oe} + R_{os}} \tag{8}$$

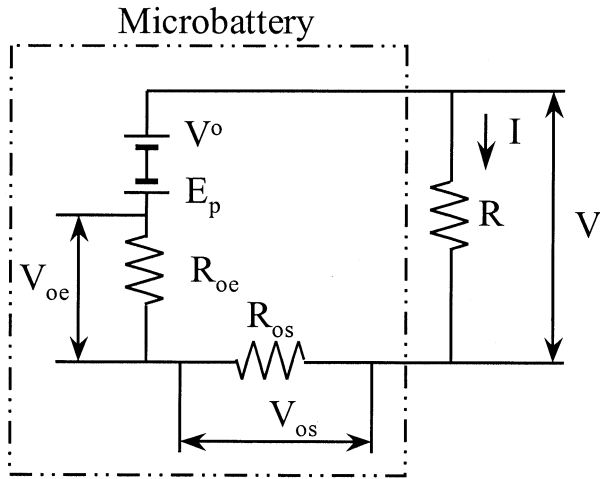


Fig. 11. Electrical model for the microbattery.

The output voltage can be obtained from (7) and (8)

$$V = r(V^o - E_p) \quad (9)$$

where r is defined as

$$r = \frac{1}{1 + \frac{R_{oe}}{R} + \frac{R_{os}}{R}} \quad (10)$$

The resistance, R_{os} , of the electrolyte is a function of the sulfuric acid conductivity, κ , and battery geometry [16] as follows:

$$R_{os} = \frac{K}{\kappa} \quad (11)$$

$$\kappa = c\Lambda = c(\Lambda^\infty - b\sqrt{c}) \quad (12)$$

where κ , K , c , Λ , Λ^∞ , and b are the conductivity of the electrolyte, the cell constant depending on battery geometries, sulfuric acid concentration, the molar conductivity of the electrolyte, the molar conductivity when c approaches 0, and a constant, respectively. After substituting (11) and (12) into (10), the resistance ratio is represented as a function of the sulfuric acid concentration as follows:

$$r = \frac{1}{1 + \frac{R_{oe}}{R} + \frac{1}{R} \left(\frac{K}{c(\Lambda^\infty - b\sqrt{c})} \right)} \quad (13)$$

It is noted from (9) and (10) that the resistance ratio increases as the external load resistance increases. Therefore, the output voltage increases under higher load resistance as observed in Figs. 7–9. It is also known from (11) that higher concentration of sulfuric acid could reduce the ohmic drop in the solution, R_{os} . As a result, r will increase and the output voltage increases as observed in Figs. 7–9. Furthermore, the transient voltage drop in Figs. 7–9 can be qualitatively explained by observing (13). Sulfuric acid concentration is reduced as r is reduced over time. These analytical models can only qualitatively explain the trend of the experimental observations. It will be very difficult, if possible, to obtain quantitative simulation results due to the fact that these electro-chemical reactions at small scale are very difficult to control and such reactions can take different pathways depending on the environment. As observed in Figs. 7–9, there

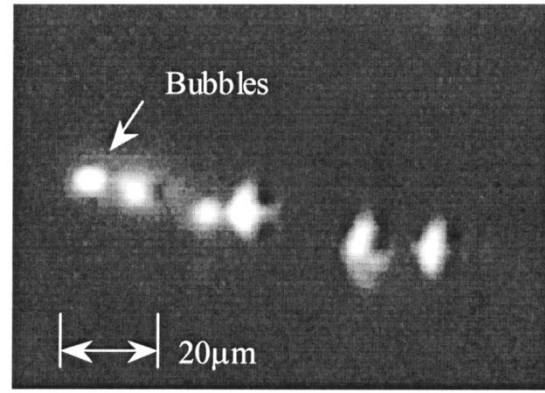


Fig. 12. Optical photo showing the bubble generation for the application of 2 M sulfuric acid. The bubbles size varies from $5 \mu\text{m}$ to $10 \mu\text{m}$. This optical photo was taken by charge-coupled device (CCD) camera of a probe station at the entrance of the cavity Fig. 2(b) after placing a droplet of $0.5 \mu\text{l}$ in front of the cavity.

TABLE II
ENERGY CAPACITY OBTAINED FROM FIGS. 7–10

H ₂ SO ₄ Concentration	Load Resistor		
	10k Ω	100k Ω	1M Ω
0.5M	17.9	18.2	14.7
1M	48.4	34.9	15.2
1.5M	117.7	82.0	21.6
2M	122.2	68.0	4.38

Energy capacity in $\mu\text{W}\cdot\text{min}$ for a droplet of $0.5\mu\text{l}$ electrolyte

are several sudden turns in the recorded experiments and are suspected to be the responses of local environmental changes such as generation of hydrogen bubbles, local flow variations and local concentration variations due to the evaporation of electrolyte. The most severe case is observed in Fig. 10 when the 2 M sulfuric acid is used in the microbattery, the output voltage is lower than the case of 1.5 M solution. It clearly disobeys the analytical model of (13) and does not follow the trend as demonstrated in Figs. 7–9. After careful characterization, it is found that hydrogen bubbles with sizes of $5\text{--}10 \mu\text{m}$ in diameter have been generated in the electrolyte as shown in Fig. 12, which is an optical photo taken by a CCD camera from a probe station at the entrance of the battery cavity [see Fig. 2(b)] after placing a droplet of $0.5 \mu\text{l}$ in the front of the cavity. This reaction is not accounted in the analytical model and appears to reduce the available output voltage. Issues involving the stability of the reagents, changing chemistry and temperature during the experiment will require further investigations.

Table II compares measured energy capacity obtained from numerical integration of data from Figs. 7–10. Energy capacity, E , of the microbattery is calculated as follows:

$$E = \int \frac{V^2}{R} dt \quad (14)$$

where V , R , and t denote the measured voltage, the load resistance and time, respectively. The general trend (except the

TABLE III
MICROBATTERY EFFICIENCIES OBTAINED FROM (9), (10), AND TABLE II

H ₂ SO ₄ Concentration	Load Resistor		
	10kΩ	100kΩ	1MΩ
0.5M	0.9	0.9	0.7
1M	1.2	0.9	0.4
1.5M	2.0	1.4	0.4
2M	1.4	0.9	0.05

Energy efficiency in %

2 M sulfuric acid electrolyte case) from Table II is that the energy capacity of the microbattery decreases when the load resistance increases, and increases when the concentration of the sulfuric acid increases. Possible reasons are discussed. Higher electrolyte concentration clearly provides higher energy capacity as discussed previously. The reason for lower measured energy capacity under higher load resistance is unclear but one possible factor is the evaporation of electrolyte. It is observed that a droplet of electrolyte will evaporate in about 30 min. Experiments with higher load resistance generate lower output current and extend the battery operation. But the energy capacity may loss over longer period of operation due to the evaporation of electrolyte such that higher load resistance results in lower capacity. The combination of 2.0 M sulfuric acid and 10 kΩ offers maximum energy capacity of 122.2 μW-min.

Another important number to be investigated is the efficiency. In this prototype system, it appears that the amount of electrolyte is the dominant factor while zinc is not going to be consumed totally. The volumetric energy density E_v can be defined as

$$E_v = V_o \frac{nF}{\text{total volume of active component}} \quad (15)$$

In practical batteries, the energy content of the actual systems is measured in terms of watt-hour (Wh) and the practical volumetric energy density is defined as

$$E_{v,pra} = \frac{Wh}{\text{volume of electrolyte}} \quad (16)$$

Therefore, the efficiency of the practical battery can be calculated as $E_{v,pra}/E_v$. Table III compares battery efficiencies obtained from (15), (16) and Table II. From Table III, it is observed that the combination of 1.5 M sulfuric acid and 10 kΩ offers maximum efficiency of 2.0% that corresponds to 72 000J per one liter of electrolyte. The general trend (except the 2 M sulfuric acid electrolyte case and 1.0 MΩ load resistor case) follows the energy capacity table. The efficiency increases as the electrolyte concentration increases before hydrogen bubbles are generated to reduce the efficiency. Moreover, the battery efficiency reduces under high load resistance probably due to longer operation time to loss efficiency due to the evaporation of electrolyte. It appears that the efficiency of these on-demand microbatteries is at least one order less than macroscale batteries. The primary reason is that most of the electrolyte is

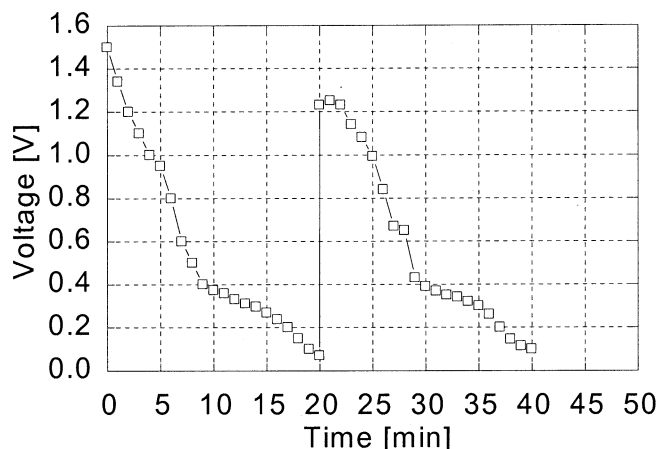


Fig. 13. Measured voltage of the microbattery with 1.0 M sulfuric acid and load resistance of 1 MΩ; the second electrolyte droplet is added after 20 min.

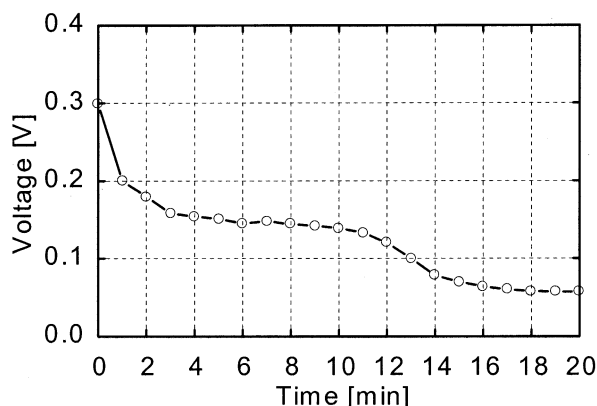


Fig. 14. Measured voltage of the microbattery with 1.0 M potassium hydroxide and load resistance of 100 kΩ.

evaporated during the process and lost to the environment. Several directions may be taken to increase the battery efficiency. First, sealing the electrolyte inside the micromachined cavity to prevent the evaporation of the electrolyte. Second, circulating the electrolyte to provide fresh solutions to be close to the electrodes. Third, other steps discussed previously from (7) to reduce the voltage drops of V_{oe} and V_{os} . One particular experiment is conducted to see the effect of adding fresh electrolyte after the first droplet of electrolyte is almost consumed. Fig. 13 shows the measured voltage of the microbattery with 1 M sulfuric acid and the load resistance of 1 MΩ. The voltage of the first droplet of the sulfuric acid varies from 1.5 V to 0.1 V during the first 20 min. After adding the second droplet, the voltage recovers back to 1.22 V and decrease afterwards in the similar pattern. Two possible effects are happening in this case. The first one is the local disturbance of the electrolyte such that fresh electrolyte can be supplied to the electrode area. The second effect is the addition of new electrolyte content to support the operation of the battery.

Fig. 14 shows the measured voltage of the microbattery with 1 M of potassium hydroxide (KOH) and the load resistance of 100 kΩ. This demonstrates the possibility of using other electrolytes to work under the same electrode system. The voltage varies from 0.3 V to 0.06 V in 20 min. It is noted that the maximum voltage of 0.3 V under 1 M of potassium hydroxide with the load

resistance of 100 k Ω is lower than that of 1.34 V of 1 M sulfuric acid and the load resistance of 100 k Ω as shown in Fig. 8.

The prototype battery is fabricated by a simple surface micromachining process. However, the operation principle can be extended to other processes. The battery can be constructed by adding a top electrode cap with built-in supports to complete the construction in Fig. 1. Furthermore, the voltage, current and capacity of the microbattery can be improved by making series or parallel battery designs and choosing other electrode/electrolyte systems.

As observed in all experiments under one single droplet of electrolyte, the voltage discharge behavior would not be desirable in practical battery operation and a circulated microfluidic system should be considered in the future development. Furthermore, it appears that the electrochemical reactions at small scale are difficult to control and they may take different pathways depending on the environment. As a result, it becomes very difficult to quantitatively characterize the experimental results as shown in Figs. 7–10. Alternatively, qualitative discussions are given in this paper in an effort to provide guidelines for future studies that may involve issues of responses of local environmental change such as generation of hydrogen bubbles, local flow variations and local concentration variations due to the evaporation of electrolyte.

Furthermore, these prototype microbatteries use various chemical electrolytes as the power sources and they are generally toxic in nature and it is not desirable for practical usage. One possible solution is to encapsulate the electrolytes with the active devices in a separate compartment. When power is needed, the boundaries of the electrolytes can be broken off for operation. The potential problems for this approach are: 1) possible degradation of the electrolyte; 2) the difficulty in encapsulating liquid for a long period of time; and 3) a proper mechanism to encapsulate liquid. Previously, a liquid encapsulation method by means of localized heating and bonding was successfully demonstrated for MEMS fabrication [17] and could be applied here for electrolyte encapsulation. However, it will still be difficult to address the chemical degradation and the storage problems for a self-contained microbattery if wet chemicals have to be stored in the system. Alternatively, a new mechanism has been demonstrated to use water (instead of toxic wet chemicals) to dissolve dry chemicals for microbattery applications [18]. Because water is benign, easy to get, and doesn't need encapsulation designs, the new on-demand and disposable microbattery could lead to great promise for practical applications.

V. CONCLUSION

A micromachined battery based on liquid electrolyte and metal electrodes for on-demand and disposal usages has been successfully demonstrated. Basic concepts of the battery operation are presented and the prototype microbattery is fabricated by using the standard surface micromachining technology. In this preliminary demonstration, sulfuric acid is chosen as the electrolyte and hydrogen peroxide is used to remove hydrogen gas. Gold is chosen as the positive electrode for collecting electrons and zinc is used as the negative electrode for offering electrons. The experimental study on the microbattery showed

that a maximum voltage of 1.5 V, energy of capacity of 122.2 $\mu\text{W}\cdot\text{min}$, and the maximum efficiency of 2% have been achieved. The microbattery also works by using potassium hydroxide as electrolyte and offers a measured maximum voltage of 0.3 V. It is foreseeable that the voltage, current and capacity of the microbattery can be improved by making series or parallel battery designs as well as by choosing other electrode/electrolyte systems. This battery can be used for on-demand and disposable MEMS devices that might require low cost, small size power sources.

ACKNOWLEDGMENT

The dicing and assembly processes of microbattery are conducted at University of California at Berkeley microfabrication laboratory.

REFERENCES

- [1] A. H. Epstein and S. D. Senturia, "Micro power from micro machinery," *Science*, vol. 276, p. 1211, May 1997.
- [2] A. H. Epstein *et al.*, "Power MEMS and microengines," in *Proc. 9th International Conference on Solid-State Sensors and Actuators*, Chicago, IL, 1997, pp. 753–756.
- [3] A. Mehra, X. Zhang, Arturo, A. Ayon, I. A. Waitz, M. A. Schmidt, and C. M. Spadaccini, "A six-wafer combustion system for a silicon micro gas turbine engine," *J. Microelectromech. Syst.*, vol. 9, pp. 517–527, Dec. 2000.
- [4] J. R. Webster, M. A. Burke, and C. H. Mastrangelo, "Electrophoresis system with integrated on-chip fluorescence detection," in *Proc. Micro Electro Mechanical Systems Workshop*, 2000, pp. 306–310.
- [5] K. B. Lee and Y.-H. Cho, "Laterally driven electro-static repulsive-force microactuators using asymmetric field distribution," *J. Microelectromech. Syst.*, vol. 10, pp. 128–136, Feb. 2001.
- [6] B. Warneke, M. Last, B. Liebowitz, and K. S. J. Pister, "Smart dust: Communicating with a cubic-millimeter computer," *IEEE Computer*, vol. 34, no. 1, pp. 44–51, 2001.
- [7] J. B. Lee, Z. Chen, M. G. Allen, and A. Rohatgi, "A miniaturized high-voltage solar cell array as an electrostatic MEMS power supply," *J. Microelectromech. Syst.*, vol. 4, pp. 102–108, Sept. 1995.
- [8] R. M. LaFollette, J. N. Harb, L. G. Salmon, and D. M. Ryan, "The performance of microscopic batteries developed for MEMS applications," in 33rd Intersociety Engineering Conference, Colorado Springs, CO, 1998, Paper IECEC-98-117.
- [9] L. G. Salmon, R. A. Barksdale, and B. R. Beachem, "Development of rechargeable microbatteries for autonomous MEMS applications," in *Proc. Solid-State Sensor and Actuator Workshop*, Hilton Head Island, SC, June 8–11, 1998, pp. 338–341.
- [10] S. D. Jones and J. R. Akridge, "Development and performance of a rechargeable thin-film solid-state microbattery," *J. Power Sources*, vol. 54, pp. 63–67, 1995.
- [11] W. C. West, J. F. Whitacre, V. White, and B. V. Ratnakumar, "Fabrication and testing of all solid-state microscale lithium batteries for microspacecraft applications," *J. Micromech. Microeng.*, vol. 12, pp. 58–62, 2002.
- [12] L. David, *Handbook of Batteries*, 2nd ed. New York: McGraw-Hill, 1995.
- [13] P. W. Atkins, *General Chemistry*. New York: Scientific American Books, 1989.
- [14] D. A. Koester, R. Mahadevan, B. Hardy, and K. W. Markus, "MUMP's design handbook," in *Revision 6.0, Cronos Integrated Microsystems: A JDS Uniphase Company*, 2001.
- [15] K. B. Lee and L. Lin, "Zinc bonding for MEMS packaging at the wafer-level," in *Proc. 2001 ASME International Mechanical Engineering Congress and Exposition*, Nov. 11–16, 2001.
- [16] W. Gilbert, *Castellan, Physical Chemistry*, 3rd ed. Reading, MA: Addison-Wesley, 1983.
- [17] Y. C. Su and L. Lin, "Localized plastic bonding for micro assembly, packaging and liquid encapsulation," in *Proc. IEEE Micro Electro Mechanical Systems Conference*, Interlaken, Switzerland, Jan. 2001, pp. 50–53.
- [18] K. B. Lee, F. Sammoura, and L. Lin, "Water activated disposable and long shelf life microbatteries," in *Proc. IEEE Micro Electro Mechanical Systems Conference*, Kyoto, Japan, Jan. 2003, pp. 387–390.



Ki Bang Lee was born in Korea, in 1962. He received the B.S., M.S., and Ph.D. degrees, all in mechanical engineering, from the Hanyang University, Seoul, Korea, and the Korea Advanced Institute of Science and Technology (KAIST), Korea, in 1985, 1987, and 2000 respectively.

He worked with Samsung Advanced Institute of Technology (SAIT), Yonginsu, Korea during 1987–2000. His last position at Samsung was a Principal Research Scientist. With Samsung and KAIST, he worked on the projects on design and fabrication of micromirror and microactuator for data storage system and hard disk drive, microactuators for tuning frequency and quality factors, design and fabrication of microgyroscope, color printer and inkjet print head, simulation and measurement of air gap between the magnetic head and tape of video cassette recorder (VCR), and noise and vibration control for refrigerators. He was a Postdoctoral Researcher of the Berkeley Sensors and Actuator Center (BSAC) at the University of California at Berkeley during 2000–2003. He has been a Research Specialist with Dr. A. P. Pisano at BSAC since October 2003. Since joining BSAC, he has been involved in the projects of Massively Parallel Post-Packaging for MEMS, Integrated Microwatt Transceivers and Water-powered Bioassay Systems that are all supported by Defense Advanced Research Projects Agency (DARPA). His research interests include MEMS (Microelectromechanical Systems); bioMEMS; micropower generation including disposable microbattery; design and fabrication of microsensors and microactuators; integrated disposable microsystems such as DNA chips, diagnostic devices, and/or labs-on-a-chip with disposable micropower; microvehicles for MEMS/bioMEMS application; microfluidic devices; optical systems on a chip.



Liwei Lin (S'92–M'93) received the M.S. and Ph.D. degrees in mechanical engineering from the University of California at Berkeley, in 1991 and 1993, respectively.

From 1993 to 1994, he was with BEI Electronics, Inc., in research and development of microsensors. From 1994 to 1996, he was an Associate Professor in the Institute of Applied Mechanics, National Taiwan University, Taiwan. From 1996 to 1999, he was an Assistant Professor at the Mechanical Engineering and Applied Mechanics Department at the University of Michigan. He joined the University of California at Berkeley in 1999 and is now an Associate Professor at Mechanical Engineering Department and Co-Director at Berkeley Sensor and Actuator Center, NSF/Industry/University research cooperative center. His research interests are in design, modeling and fabrication of microstructures, microsensors and microactuators as well as mechanical issues in microelectromechanical systems including heat transfer, solid/fluid mechanics and dynamics. He holds eight U.S. patents in the area of MEMS.

Dr. Lin is the recipient of the 1998 NSF CAREER Award for research in MEMS Packaging and the 1999 *ASME Journal of Heat Transfer* Best Paper Award for his work on microscale bubble formation. He served as Chairman of the Micromechanical Systems Panel of the ASME Dynamic Systems and Control Division in 1997 and 1998 and led the effort in establishing the MEMS subdivision in ASME and is currently the Vice Chairman of the Executive Committee. He is a Member of the American Society of Mechanical Engineers (ASME).